Dielectric optical elements for surface plasmons

Andreas Hohenau, Joachim R. Krenn, Andrey L. Stepanov, Aurelien Drezet, Harald Ditlbacher, Bernhard Steinberger, Alfred Leitner, and Franz R. Aussenegg

Institute for Physics and Erwin Schrödinger Institute for Nanoscale Research, Karl-Franzens-University Graz, A-8010 Graz, Austria

Received October 14, 2004

Basic optical elements for surface plasmons are fabricated and their functionality (focusing, refraction, and total internal reflection) is demonstrated experimentally. The optical elements consist of dielectric structures of defined geometry on top of a gold film. The working principle of these structures is discussed on the basis of calculated surface plasmon dispersion relations. © 2005 Optical Society of America

OCIS codes: 240.6680, 130.2790, 230.3120.

The recent rapid increase in the number of publications on surface plasmon (SP) photonics demonstrates the growing interest in using SPs as signal carriers in nanoscale two-dimensional optical circuits. So far, many different concepts have been suggested, including photonic bandgap structures,[1] metal stripes in a dielectric environment,[2] Bragg mirrors composed of metal particles on a metal surface,[3] grooves[4] and ridges[5] in metal surfaces, and metal particle waveguides.[6,7] Although basic SP guiding in straight structures can be demonstrated experimentally,[8] only a few structures (e.g., Bragg reflectors[3]) are known to efficiently guide SPs around corners or can be used for SP focusing,[9] which is essential for all thinkable applications of SPs in photonic circuits.

We suggest a different approach to the challenging task of controlling SP propagation: the use of dielectric thin-film structures on top of a metal surface. In this Letter we demonstrate that SP focusing, refraction, and reflection can be achieved by such dielectric structures of controlled geometric shapes.

In conventional optics the realization of simple optical elements such as lenses, prisms, and waveguides relies on a geometrically defined spatial change in the velocity of light. This change is formally described by a shift of the light dispersion relation at a given frequency. For SPs the same principle can be applied, so for the realization of any SP optical elements, one needs a controlled spatial variation of the SP velocity, i.e., a shift of the SP dispersion relation.

To explore the possibilities of the realization of an appropriate modification in the SP dispersion relation, we analyze the situation considering a planar metal film between two dielectric media. This system is theoretically simple and to a good approximation experimentally accessible. The analytical, implicit form of the SP dispersion relation is given by[10]

$$1 + r^p_{1,2} r^p_{2,3} \exp(2ik_{z,2}d) = 0,$$

with

$$r^p_{i,j} = \left(\frac{k_{z,i}}{\epsilon_i} - \frac{k_{z,j}}{\epsilon_j}\right) \Bigg/ \left(\frac{k_{z,i}}{\epsilon_i} + \frac{k_{z,j}}{\epsilon_j}\right), \quad k_{z,i} = (\epsilon_i k_0^2 - k_x^2)^{1/2}, \tag{1}$$

and can be solved numerically.[11] (ϵ_1 is the dielectric function of the substrate, ϵ_3 is that of the superstrate, ϵ_2 is that of the metal. k_0 is the vacuum wave-number of light, and k_x is the wave number component parallel to the interfaces.) This relation yields two physically relevant SP modes, both transverse magnetic in character.[11] The *s* mode (*a* mode) has the maximum of the electromagnetic field on the air–metal (glass–metal) interface, and the magnetic fields on the two interfaces of the metal film are in phase (counterphase).

The different options for modifying the dispersion relation of the SP modes are [see Eq. (1)] changing the metal dielectric function (ϵ_2), the metal film thickness (d), the dielectric function of one or both of the two dielectrics (ϵ_1, ϵ_3), and any combination of the above.

In the following we focus on the effect of the top dielectric medium on the SP dispersion relation. Figure 1 shows examples of the calculated dispersion relations of a 50-nm-thick gold film on glass ($\epsilon_1 = 2.25$) for different dielectric functions of the top dielectric medium (ϵ_3). An increase in ϵ_3 leads to a shift to larger SP wave vectors (lower SP velocity) for both SP

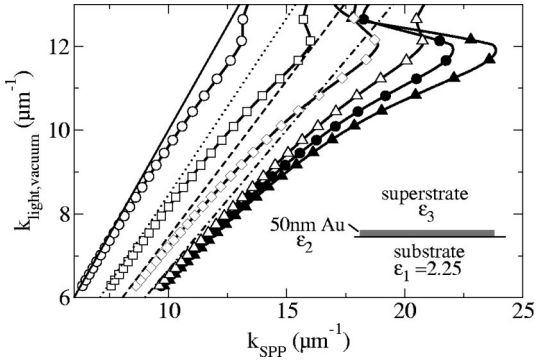

Fig. 1. Calculated dispersion relation of the two SP modes on a 50-nm thin gold film (dielectric function from Johnson and Christy[12]) between a glass substrate ($\epsilon_1 = 2.25$) and a superstrate with $\epsilon_3 = 1$ (circles), $\epsilon_3 = 1.4$ (squares), $\epsilon_3 = 1.8$ (diamonds), and $\epsilon_3 = 2.25$ (triangles). The open symbols refer to the *s* mode SP, and the filled symbols refer to the *a*-mode SP (only plotted for $\epsilon_3 = 1$ and 2.25). For comparison, the light lines for a medium with $\epsilon = 1$ (solid line), $\epsilon = 1.4$ (dotted line), $\epsilon = 1.8$ (dashed line), and $\epsilon = 2.25$ (dashed–dotted line) are drawn.

0146-9592/05/080893-3/$15.00

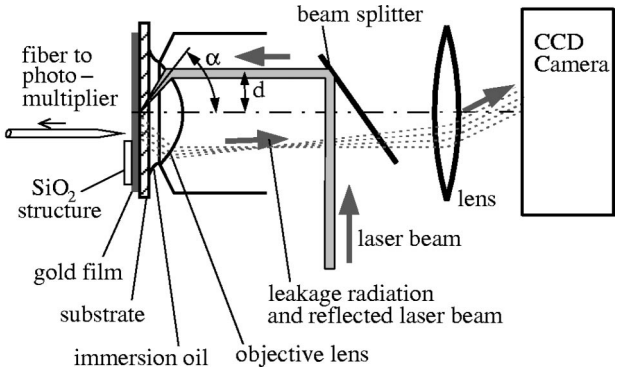

Fig. 2. Sketch of the experimental setup.

modes (see Fig. 1). In analogy to conventional optics it should therefore be possible to fabricate lenses, beam splitters, and waveguides for SP modes if this shift in the dispersion relation is localized to regions of corresponding geometric shape on the metal surface.

For the experimental demonstration of such SP optical elements we investigate the influence of a laterally confined dielectric layer on top of the metal surface on SPs. This approach is justified since SPs, because of their evanescent character, are influenced strongly by the immediate vicinity of the interface.

The basic structure of our samples is shown in Fig. 2. A 50-nm gold film is deposited onto a 155-μm-thick glass cover slide by vacuum vapor deposition. The dielectric structures of SiO_2 on top of the gold film are produced by electron-beam lithography[13]: First the sample gets spin cast with electron-beam resist, and then it is exposed by a focused electron beam. During the following development process, the resist is removed in the exposed areas. The sample is then covered with a thin layer of SiO_2 by electron-beam evaporation, and finally the SiO_2 together with the resist is removed from the unexposed areas by a lift-off process. The height of the SiO_2 layer for all the samples is below the cutoff thickness of the waveguide modes in the SiO_2 layer (150 nm).

To observe the effects of the dielectric structures on top of the gold film on the SPs, we look at either the leakage radiation[14,15] or the optical near field of locally launched SPs. Both methods are integrated in the same experimental setup (Fig. 2).

The SPs are locally excited by a laser beam (wavelength of 800 nm, FWHM $\approx$ 0.5 mm) entering an oil-immersion objective (60×, 1.4 numerical aperture) eccentrically (see Fig. 2). The objective focuses the laser beam onto the metal–glass interface under a mean angle α, which is controlled by distance d between the laser beam and the optical axis of the objective. If α is adjusted to a certain value above the angle of total internal reflection, a SP on the gold–air interface can be locally excited in analogy to the excitation scheme in the Kretschmann–Räther configuration.[10] The excited SP beam has a FWHM of 5 μm (determined by the size of the diffraction-limited laser focus) and propagates parallel to the plane of incidence away from the launching region. By propagating, the SP emits leakage radiation[14,15] that is collected by the oil-immersion objective and imaged onto a CCD camera. A propagating plasmon beam appears on the CCD image as a bright stripe on an otherwise dark background.

To ensure the SP character of the images acquired by the CCD, we also perform optical near-field measurements with a photon scanning tunnel microscope. A dielectric fiber tip with a tip diameter of approximately 100 nm is scanned over the sample surface and kept at a constant distance by shear force feedback. The tip scatters part of the optical near field into propagating modes of the fiber. A photomultiplier attached to the far end of the fiber records an intensity level that is proportional to the electric field intensity at the fiber tip.[16]

Figure 3 shows the leakage radiation and optical near-field images of a locally launched plasmon interacting with a triangular and a circular 40-nm-high SiO_2 structure on top of the 50-nm-thick gold film. These elements affect the SP propagation in complete analogy to the effects of their three-dimensional counterparts (prism and sphere) on light: Refraction, reflection, and focusing can be achieved. Evaluated by Snell's law, the observed SP refraction (Fig. 3) is characterized by a SP effective refractive index $n_{\mathrm{eff}}^{\mathrm{SP}}$ of 1.1 ± 0.05 for the SiO_2 layer ($n_{\mathrm{eff}}^{\mathrm{SP}}$ is assumed to be 1 in the uncovered region). For a 90-nm-thick SiO_2 layer we find $n_{\mathrm{eff}}^{\mathrm{SP}} = 1.2 \pm 0.05$, and the analog effect on total internal reflection is demonstrated for a SP at angles of incidence α_i (relative to the normal of the reflecting edge) up to $\approx 56°$ (see Fig. 4 for $\alpha_i \approx 72°$).

For all the structures shown above, the SP still emits leakage radiation into the glass substrate. To

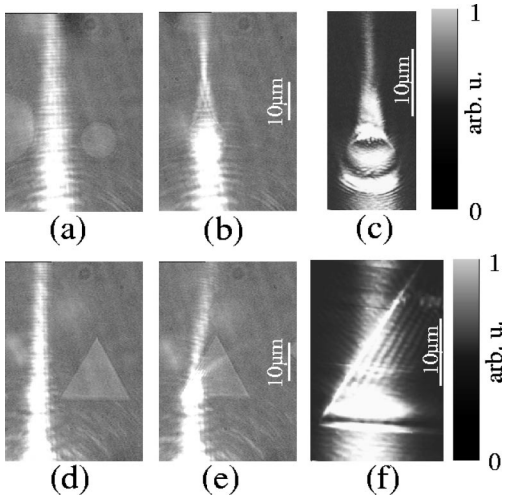

Fig. 3. Locally launched SP beam interacting with (b), (c) a cylindrical and (e), (f) a triangular SiO_2 structure. The sample is weakly illuminated so that the outlines of the SiO_2 structure can be recognized in the leakage images [(a), (b), (d), (e)]. For comparison, the leakage radiation images of the freely propagating beam beside the structures are presented in (a) and (d). (b) and (e) The leakage radiation images of the beam interacting with the SiO_2 structures, (c) and (f) The corresponding optical near-field images. For the circular structure focusing and for the triangular structure, refraction and weak reflection of the SP beam are observed. The fringes parallel to the prism edge in (f) result from the interference of the incident and the reflected SP beam.

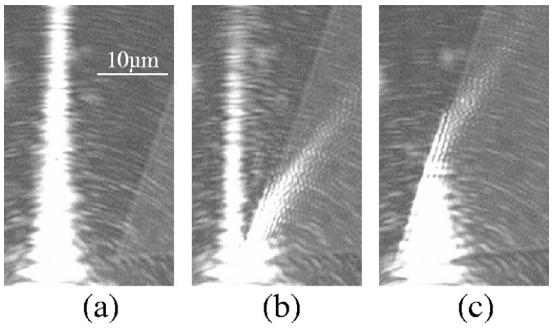

Fig. 4. Leakage radiation images of total internal reflection of a locally launched SP. The sample is weakly illuminated so that the outlines of the SiO_2 structure can be recognized on the right side of the images as part of a triangle. (a) The freely propagating SP beam beside the triangle. Keeping the excitation at a constant position, the triangle is moved into the SP beam (b) until the whole beam is totally reflected from the upper edge of the triangle (c).

overcome this, the gold film thickness could be increased to more than ~70 nm, which practically eliminates leakage radiation and edge scattering into the substrate. Further, if the SP dispersion relation at a given frequency lies to the right of the substrate and superstrate light line (e.g., the s mode for $\epsilon_3 = 1.8$ and $\epsilon_1 = 2.25$ above $k_{\text{light}} = 10.7\ \mu\text{m}^{-1}$; Fig. 1), the SP cannot emit leakage radiation. In this case, total internal reflection of the SP without leakage radiation and edge scattering occurs, provided that the k_{SP} component parallel to the edge is larger than k_{light} in both the substrate and the superstrate. It therefore should be possible to fabricate nonleaky SP waveguides by placing thin dielectric structures on top of a metal film in analogy to dielectric light waveguides.

In conclusion, we have shown that spatially confined dielectric thin-film structures allow the fabrication of optical elements such as prisms and lenses for surface plasmons. We demonstrated the functionality of these elements for an s-mode surface plasmon experimentally. Additionally, we found for surface plasmons an effect similar to total internal reflection. On the basis of these results, criteria to fabricate nonleaky surface plasmon waveguides were specified.

We acknowledge the European Union under projects FP6 NMP4-CT-2003-505699 and FP6 2002-IST-1-507879 and the Austrian Science Foundation for financial support. A. Hohenau's e-mail address is andreas.hohenau@uni-graz.at.

References

1. S. I. Bozhevolnyi, V. S. Volkov, K. Leosson, and A. Boltasseva, Appl. Phys. Lett. **79**, 1076 (2001).
2. P. Berini, Opt. Express **7**, 329 (2000), http://www.opticsexpress.org.
3. H. Ditlbacher, J. R. Krenn, G. Schider, A. Leitner, and F. R. Aussenegg, Appl. Phys. Lett. **81**, 1762 (2002).
4. D. F. P. Pile and D. K. Gramotnev, Opt. Lett. **29**, 1069 (2004).
5. T. Yatsui, M. Kourogi, and M. Ohtsu, Appl. Phys. Lett. **79**, 4583 (2001).
6. M. Brongersma, J. Hartman, and H. A. Atwater, Phys. Rev. B **62**, 16356 (2000).
7. M. Quinten, A. Leitner, J. Krenn, and F. Aussenegg, Opt. Lett. **23**, 1331 (1998).
8. J. Krenn, B. Lamprecht, H. Ditlbacher, G. Schider, M. Salerno, A. Leitner, and F. Aussenegg, Europhys. Lett. **60**, 663 (2003).
9. J. Krenn, H. Ditlbacher, G. Schider, A. Hohenau, A. Leitner, and F. Aussenegg, J. Microsc. **209**, 167 (2003).
10. H. Raether, *Surface Plasmons on Smooth and Rough Surfaces and on Gratings*, Vol. 111 of Springer Tracts in Modern Physics (Springer-Verlag, Berlin, 1988).
11. J. J. Burke, G. I. Stegeman, and T. Tamir, Phys. Rev. B **33**, 5186 (1986).
12. P. B. Johnson and R. W. Christy, Phys. Rev. B **6**, 4370 (1972).
13. M. A. McCord and M. J. Rooks, *Handbook of Microlithography, Micromachining and Microfabrication* (SPIE Press, Bellingham, Wash., 1997).
14. B. Hecht, H. Bielefeldt, L. Novotny, Y. Inouye, and D. Phol, Phys. Rev. Lett. **77**, 1889 (1996).
15. A. Bouhelier, T. Huser, H. Tamaru, H. Güntherodt, D. Pohl, F. Baida, and D. van Labeke, Phys. Rev. B **63**, 155404 (2001).
16. A. Dereux, C. Girard, and J. C. Weeber, J. Chem. Phys. **112**, 7775 (2000).